Available online at www.sciencedirect.com
ScienceDirect
Journal of Organometallic Chemistry 692 (2007) 1661–1671
Journal of Organometallic Chemistry
www.elsevier.com/locate/jorganchem

Mono and dinuclear iridium, rhodium and ruthenium complexes containing chelating carboxylato pyrazine ligands: Synthesis, molecular structure and electrochemistry

Padavattan Govindaswamy [a], Bruno Therrien [a,*], Georg Süss-Fink [a], Petr Štěpnička [b,*], Jiří Ludvík [c]

[a] Institut de Chimie, Université de Neuchâtel, Case postale 158, CH-2009 Neuchâtel, Switzerland
[b] Charles University, Faculty of Science, Department of Inorganic Chemistry, Hlavova 2030, CZ-12840 Prague 2, Czech Republic
[c] J. Heyrovský Institute of Physical Chemistry, Academy of Sciences of the Czech Republic, Dolejškova 3, CZ-18223 Prague, Czech Republic

Received 10 November 2006; received in revised form 8 December 2006; accepted 18 December 2006
Available online 11 January 2007

Abstract

The mononuclear complexes $[(\eta^5\text{-}C_5Me_5)IrCl(L^1)]$ (**1**), $[(\eta^5\text{-}C_5Me_5)RhCl(L^1)]$ (**2**), $[(\eta^6\text{-}p\text{-}Pr^iC_6H_4Me)RuCl(L^1)]$ (**3**) and $[(\eta^6\text{-}C_6Me_6)RuCl(L^1)]$ (**4**) have been synthesised from pyrazine-2-carboxylic acid (HL^1) and the corresponding complexes $[\{(\eta^5\text{-}C_5Me_5)IrCl_2\}_2]$, $[\{(\eta^5\text{-}C_5Me_5)RhCl_2\}_2]$, $[\{(\eta^6\text{-}p\text{-}Pr^iC_6H_4Me)RuCl_2\}_2]$, and $[\{(\eta^6\text{-}C_6Me_6)RuCl_2\}_2]$, respectively. The related dinuclear complexes $[\{(\eta^5\text{-}C_5Me_5)IrCl\}_2(\mu\text{-}L^2)]$ (**5**), $[\{(\eta^5\text{-}C_5Me_5)RhCl\}_2(\mu\text{-}L^2)]$ (**6**), $[\{(\eta^6\text{-}p\text{-}Pr^iC_6H_4Me)RuCl\}_2(\mu\text{-}L^2)]$ (**7**) and $[\{(\eta^6\text{-}C_6Me_6)RuCl\}_2(\mu\text{-}L^2)]$ (**8**) have been obtained in a similar manner from pyrazine-2,5-dicarboxylic acid (H_2L^2). Compounds isomeric to the latter series, $[\{(\eta^5\text{-}C_5Me_5)IrCl\}_2(\mu\text{-}L^3)]$ (**9**), $[\{(\eta^5\text{-}C_5Me_5)RhCl\}_2(\mu\text{-}L^3)]$ (**10**), $[\{(p\text{-}Pr^iC_6H_4Me)RuCl\}_2(\mu\text{-}L^3)]$ (**11**) and $[\{(\eta^6\text{-}C_6Me_6)RuCl\}_2(\mu\text{-}L^3)]$ (**12**), have been prepared by using pyrazine-2,3-dicarboxylic acid (H_2L^3) instead of H_2L^2. The molecular structures of **2** and **3**, determined by X-ray diffraction analysis, show the pyrazine-2-carboxylato moiety to act as an *N*,*O*-chelating ligand, while the structure analyses of **5**–**7**, confirm that the pyrazine-2,5-dicarboxylato unit bridges two metal centres. The electrochemical behaviour of selected representatives has been studied by voltammetric techniques.

Keywords: Dinuclear complexes; Iridium; Rhodium; Ruthenium; Pyrazinecarboxylato ligands; Electrochemistry

1. Introduction

Formation of supramolecular architectures via self-assembly of transition metal complex units is dominated by square-planar metal coordination geometries. Pioneered by Fujita in 1990 [1], and later exploited by other groups [2], the combination of 90° coordination building blocks and linear ligands leading to square and rectangular networks has been extensively studied. A few years later, the same approach was used to generate three-dimensional networks [3]. So far a multitude of two- and three-dimensional structures incorporating transition metals with square-planar geometry have been synthesised [4]. In the search for new building blocks for the synthesis of supramolecular materials with interesting properties, there is an increasing interest in using transition metal complexes with octahedral geometry [5]. Recently, Severin has constructed a series of macrocycles and cages by connecting $(\eta^5\text{-}C_5Me_5)M(III)$ (M = Ir, Rh) or (η^6-arene)Ru(II) fragments by multifunctional ligands [6]. Self-assembly of such half-sandwich complex units with 3-hydroxy-2-pyridone in the presence of a base (Cs_2CO_3) led to the formation of trinuclear metallacrowns [7]; this work was inspired from the trinuclear metallacrown $[(\eta^5\text{-}C_5Me_5)Rh(9\text{-methyladenyl})]_3[O_3SCF_3]_3 \cdot 6H_2O$ synthesised by Fish in the early 1990s [8].

* Corresponding authors. Tel.: +41 32 718 2499; fax: +41 32 718 2511 (B. Therrien).
E-mail addresses: bruno.therrien@unine.ch (B. Therrien), stepnic@natur.cuni.cz (P. Štěpnička).

0022-328X/$ - see front matter © 2007 Elsevier B.V. All rights reserved.
doi:10.1016/j.jorganchem.2006.12.040

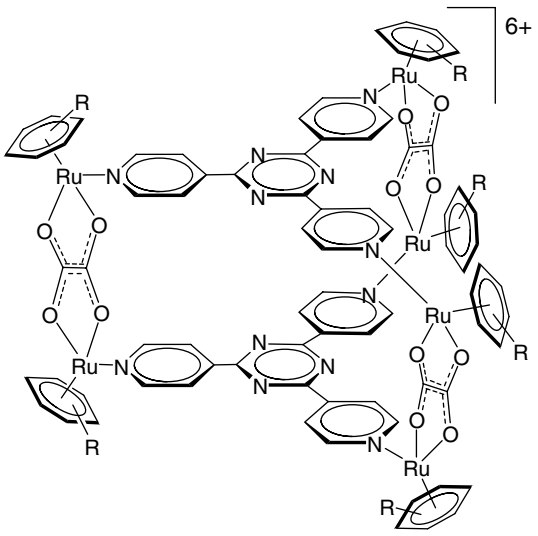

Recently we have shown the cationic triangular metallo-prisms $[(\eta^6\text{-arene})_6Ru_6(4\text{-tpt})_2(\mu_2\text{-}C_2O_4)_3]^{6+}$ (arene = *p*-$Pr^iC_6H_4Me$, C_6Me_6: 4-tpt = 2,4,6-tri(pyridin-4-yl)-1,3,5-triazine) containing bridging oxalato ligands to have a double-helical chirality [9]. Therefore, in search of new dinuclear bridging units, we have synthesised a series of dinuclear pyrazine carboxylato complexes incorporating $(\eta^5\text{-}C_5Me_5)M(III)$ (M = Ir, Rh) or $(\eta^6\text{-arene})Ru(II)$ fragments. The different pyrazine carboxylato derivatives used in the present study are shown in Scheme 1. Although it turned out that with these systems and with 4-tpt building blocks triangular metallo-prisms did not form, the new ruthenium, iridium and rhodium pyrazine carboxylato complexes are interesting in their own right from a synthetic, structural and electrochemical point of view. The structure of several representatives has been determined by X-ray structure analysis, and the redox behaviour of the complexes studied by voltammetric methods.

2. Results and discussion

2.1. Syntheses and characterisation

The dinuclear pentamethylcyclopentadienyl complexes $[\{(\eta^5\text{-}C_5Me_5)MCl_2\}_2]$ (M = Ir, Rh) and the arene ruthenium complexes $[\{(\eta^6\text{-arene})RuCl_2\}_2]$ (arene = *p*-$Pr^iC_6H_4Me$, C_6Me_6) react with pyrazine-2-carboxylic acid

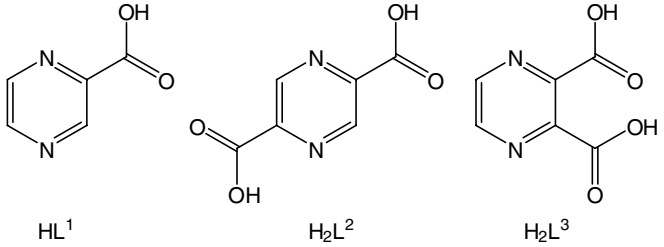

Scheme 1.

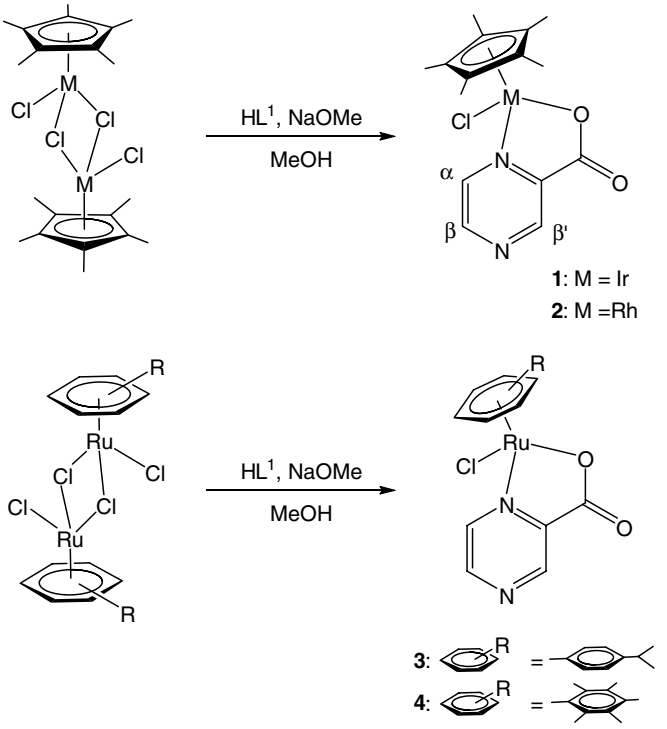

Scheme 2. Synthesis of complexes **1**–**4**.

(HL^1) in the presence of sodium methoxide in methanol to form the neutral mononuclear pentamethylcyclopentadienyl iridium and rhodium complexes $[(\eta^5\text{-}C_5Me_5)IrCl(L^1)]$ (**1**), $[(\eta^5\text{-}C_5Me_5)RhCl(L^1)]$ (**2**) and the arene ruthenium complexes $[(\eta^6\text{-arene})RuCl(L^1)]$ (arene = *p*-$Pr^iC_6H_4Me$: **3**, arene = C_6Me_6: **4**) (Scheme 2). The complexes **1**–**4** are orange-yellow, non-hygroscopic, air-stable and shiny orange crystalline solids. They are sparingly soluble in methanol, chloroform, soluble in dichloromethane, acetone, acetonitrile, and insoluble in hexane and diethyl ether.

The infrared spectra of **1**–**4** show the presence of a ν(COO) band in the range 1645–1660 cm^{-1}, which is comparable with the literature values [10]. The ^1H NMR spectra of complexes **1**, **2**, and **4** exhibit a strong methyl signal at $\delta = 1.68$, 1.70 and 2.18, respectively, for the pentamethylcyclopentadienyl and hexamethylbenzene methyl groups. The ^1H NMR spectrum of **3** exhibits two doublets for the diastereotopic methyl protons of the isopropyl group, since the ruthenium atom is stereogenic due to the coordination of four different ligator atoms. Likewise, the diastereotopic CH protons of the *p*-cymene ligand give rise to four doublets observed between $\delta = 5.49$–5.69. A septet at $\delta = 2.89$ is observed for the CH proton of the isopropyl group. The α-proton (see Scheme 1) of the pyrazine moiety in **1**–**4** appears as a doublet at $\delta \approx 8.85$. The H_β and $H_{\beta'}$ appear as double doublet and a doublet at $\delta \approx 8.65$ and 9.15 ppm, respectively.

The reaction of the dimeric chloro complexes $[\{(\eta^5\text{-}C_5Me_5)MCl_2\}_2]$ (M = Ir or Rh) and $[\{(\eta^6\text{-arene})RuCl_2\}_2]$ (arene = *p*-$Pr^iC_6H_4Me$, C_6Me_6) with pyrazine-2,5-dicar-

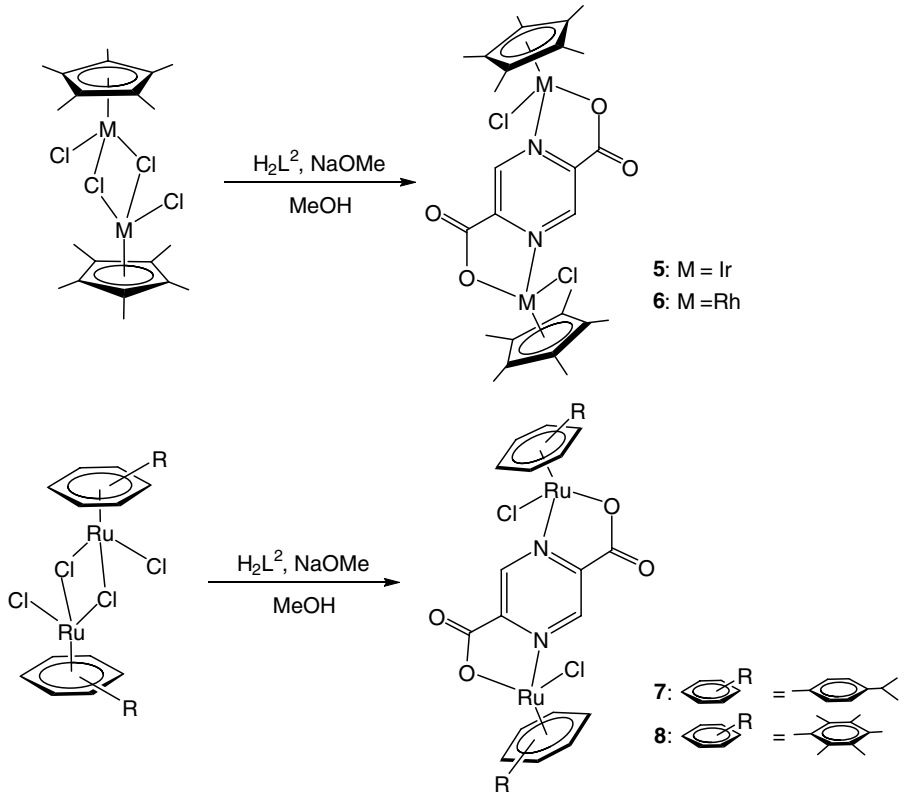

Scheme 3. Synthesis of complexes **5**–**8**.

boxylic acid (H_2L^2) at the appropriate molar ratio in presence of NaOMe in methanol results in the formation of the orange coloured, air-stable dinuclear complexes $[\{(\eta^5\text{-}C_5Me_5)IrCl\}_2(\mu\text{-}L^2)]$ (**5**), $[\{(\eta^5\text{-}C_5Me_5)RhCl\}_2(\mu\text{-}L^2)]$ (**6**), $[\{(\eta^6\text{-}p\text{-}Pr^iC_6H_4Me)RuCl\}_2(\mu\text{-}L^2)]$ (**7**) and $[\{(\eta^6\text{-}C_6Me_6)\text{-}RuCl\}_2(\mu\text{-}L^2)]$ (**8**) (Scheme 3). In the IR spectra of **5**–**8** a strong band appears at around 1660 cm^{-1} due to the ν(COO) vibration of the pyrazine-2,5-dicarboxylato ligand (L^2) [10]. ^1H NMR spectra of **5**–**8** exhibit a sharp singlet between $\delta = 8.98$ and 9.31, which can be assigned to the pyrazine protons, while the C_5Me_5 or C_6Me_6 protons appear at δ 1.70 for **5**–**6** and at $\delta = 2.17$ for complex **8**. Complex **7** exhibits only one characteristic set of doublets at $\delta = 1.32$ and 1.29, and a septet at $\delta = 2.95$ for the isopropyl protons. This observation suggests that despite the presence of the *cis* and *trans* isomers in the crystal packing of **7**, in solution the isomerisation is fast on the NMR time-scale.

The analogous reaction between $[\{(\eta^5\text{-}C_5Me_5)MCl_2\}_2]$ (M = Ir or Rh) and $[\{(\eta^6\text{-arene})RuCl_2\}_2]$ (arene = *p*-$Pr^iC_6H_4Me$, C_6Me_6) and pyrazine-2,3-dicarboxylic acid (H_2L^3) in methanol in the presence of NaOMe yields the neutral bis(*N*,*O*-chelated) dinuclear complexes of the types $[\{(\eta^5\text{-}C_5Me_5)MCl\}_2(\mu\text{-}L^3)]$ (M = Ir: **9**, M = Rh: **10**) and $[\{(\eta^6\text{-arene})RuCl\}_2(\mu\text{-}L^3)]$ (arene = *p*-$Pr^iC_6H_4Me$: **11**, arene = C_6Me_6: **12**) (Scheme 4). While **11** and **12** are soluble in acetonitrile, **9** and **10** are insoluble even in acetonitrile and dimethylsulfoxide, hence, they could be characterised only by their IR, MS and micro-analytical data.

The IR spectra of complexes **9**–**12** exhibit two bands for the ν(COO) vibration around 1680 and 1660 cm^{-1}. This may be explained by the asymmetry induced by the twist in the ligand as a result of the coordination. The ^1H NMR spectrum of **11** in CD_3CN shows a singlet resonance for L^3 at $\delta = 9.12$ and two multiplets for aromatic *p*-cymene moiety centred at δ 5.76 and 5.59, respectively. The methyl protons of isopropyl group resonate at $\delta = 1.28$ ppm, as two doublets due to the diastereotopic nature of the isopropyl group. Two singlets are observed for complex **12**, the first one at $\delta = 8.58$ being due to the L^3 protons and the second one at $\delta = 2.09$ due to the hexamethylbenzene protons.

The molecular structure of mononuclear carboxylato pyrazine complexes has been established by single-crystal X-ray structure analysis of the two representatives **2** and **3**. Both complexes show a typical piano-stool geometry with the metal centre coordinated by the aromatic ligand, a terminal chloride and a chelating *N*,*O*-ligand (see Figs. 1 and 2). The distance between the Rh atom and the centre of the $\eta^5\text{-}C_5Me_5$ ligand in **2** is 1.764 Å, while the distance between the Ru atom and the centre of the C_6H_4 aromatic ring of the $\eta^6\text{-}p\text{-}Pr^iC_6H_4Me$ ligand in **3** is 1.669(7) Å. The Rh(1)–N(1) bond distance [2.111(5) Å] in **2** is comparable to that in **3** [Ru(1)–N(1) = 2.095(5) Å] while the Rh(1)–O(1) bond distance [2.145(4) Å] in **2** is slightly longer than the Ru(1)–O(1) distance [2.096(5) Å] in **3**. There is no significant difference in the M–Cl bond lengths in **2** and **3** [average 2.407 Å] and the values compare well with the

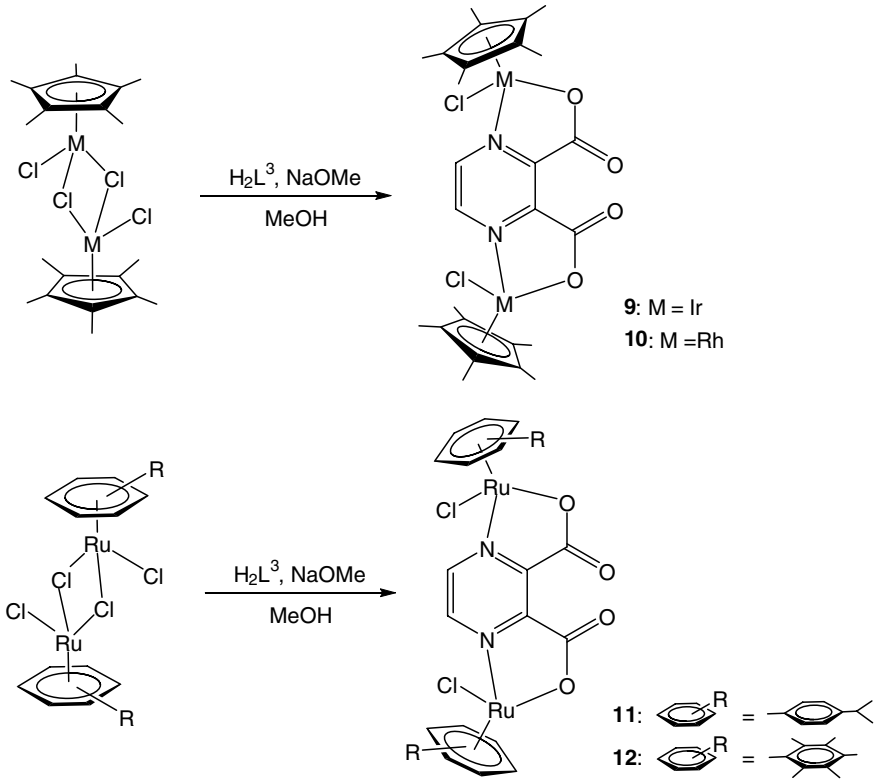

Scheme 4. Synthesis of complexes **9**–**12**.

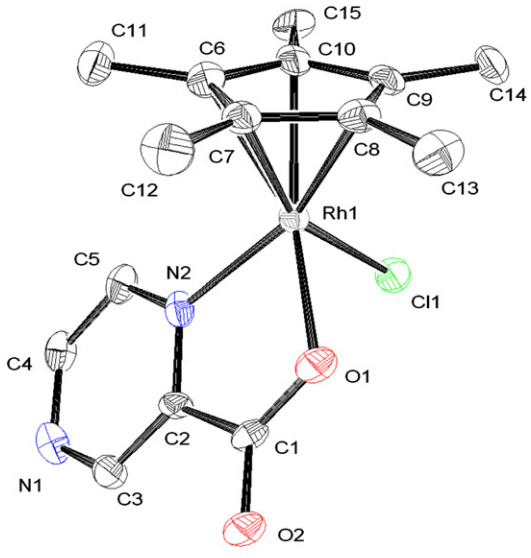

Fig. 1. ORTEP diagram of complex **2** with 50% probability thermal ellipsoids. Hydrogen atoms are omitted for clarity. Selected bond lengths (Å) and angles (°): Rh(1)–Cl(1) 2.4100(16), Rh(1)–N(2) 2.111(5), Rh(1)–O(1) 2.145(4); N(2)–Rh(1)–Cl(1) 86.45(14), N(2)–Rh(1)–O(1) 78.0(2), O(1)–Rh(1)–Cl(1) 91.81(15).

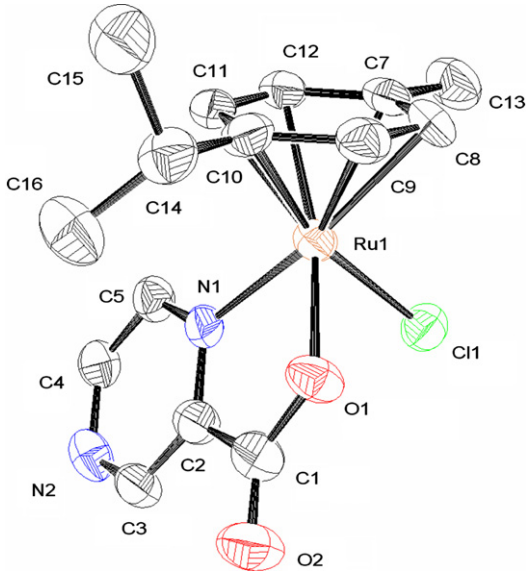

Fig. 2. ORTEP diagram of complex **3** with 50% probability thermal ellipsoids. Hydrogen atoms are omitted for clarity. Selected bond lengths (Å) and angles (°): Ru(1)–N(1) 2.095(5), Ru(1)–Cl(1) 2.405(2), Ru(1)–O(1) 2.096(5); N(1)–Ru(1)–Cl(1) 84.27(18), N(1)–Ru(1)–O(1) 77.6(2), O(1)–Ru(1)–Cl(1) 86.29(17).

reported values [11,12]. The O(1)–Rh(1)–N(2) bond angles of complex **2** [78.0(2)°] are similar to that of complex **3** [O(1)–Ru(1)–N(1) = 77.6(2)°].

In the mononuclear complexes **1**–**4**, the metal centre is stereogenic. However, since none of the ligand contains a chiral information, **1**–**4** are obtained as racemic mixtures. While the single crystal X-ray analysis of **3** (space group $P2_1/n$) shows the two expected enantiomers in the same crystal, the X-ray analysis of **2** (space group $P2_12_12_1$) reveals an enantiopure crystal containing only the (*R*)-enantiomer. However, the CD (circular dichroism) spec-

trum of a dichloromethane solution of a single-crystal of **2** shows no optical activity, suggesting fast racemisation in solution.

The complexes **5** and **6** crystallise in the space group $P2_1/n$, while complex **7** crystallises in the space group $C2/c$. ORTEP drawings with the atom labelling scheme for the complexes **5**–**7** are shown in Figs. 3–5 together with selected bond lengths and angles. Complexes **5**–**7** contain two metal centres (Ir(III), Rh(III) or Ru(II)) bonded to a η^5-C_5Me_5 or η^6-*p*-Pr^{i}C$_6$H$_4$Me ligands, respectively, which are bridged by the dianionic $(L^2)^{2-}$ ligand through its oxygen and nitrogen atoms. The distance between the iridium atom and the centre of the η^5-C_5Me_5 ring is 1.770 Å in **5**, whereas the corresponding Rh–C_5Me_5 distance in **6** is 1.765 Å. These bond lengths are comparable to those in the related complex cations $[(\eta^5\text{-}C_5Me_5)IrCl(C_5H_4N\text{-}2\text{-}CH{=}N\text{–}C_6H_4\text{-}p\text{-}X)]^+$, where X = NO_2, and Cl [14]. The Ir(1)–N(1) and Rh(1)–N(1) bond lengths are 2.107(3) Å for complex **5** and 2.132(2) Å for complex **6**, which is in accordance with the reported complexes $[(\eta^5\text{-}C_5Me_5)IrCl(S\text{-}1\text{-phenylethylsalicylaldiimine})]$ [2.121(3) Å] and $[(\eta^5\text{-}C_5Me_5)RhCl(S\text{-}1\text{-phenylethylsalicylaldiimine})]$ [2.136(3) Å] [12a]. The M–Cl bond lengths are 2.4048(13) Å (in **5**) and 2.4086(8) Å (in **6**), which are closely similar to reported poly-pyridyl rhodium complex cation $[(\eta^5\text{-}C_5Me_5)RhCl(4'\text{-phenyl-}2,2':6',2''\text{-terpyridine})]^+$ [2.3984 (1) Å] [13].

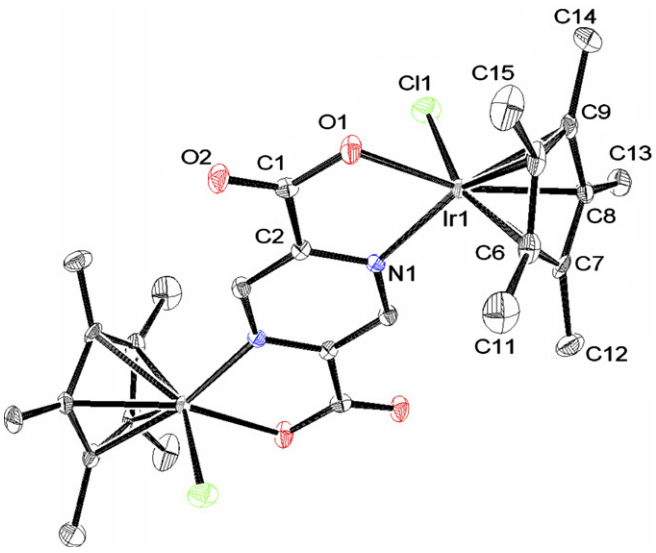

Fig. 3. ORTEP diagram of complex **5** with 50% probability thermal ellipsoids. Hydrogen atoms are omitted for clarity. Selected bond lengths (Å) and angles (°): Ir(1)–Ir(1)^i 6.9751(6), Ir(1)–N(1) 2.107(3), Ir(1)–O(1) 2.099(3), Ir(1)–Cl(1) 2.4048(13); O(1)–Ir(1)–Cl(1) 87.49(11), O(1)–Ir(1)–N(1) 77.19(13), N(1)–Ir(1)–Cl(1),83.30(11) ($i = 1 - x, -y, -z$).

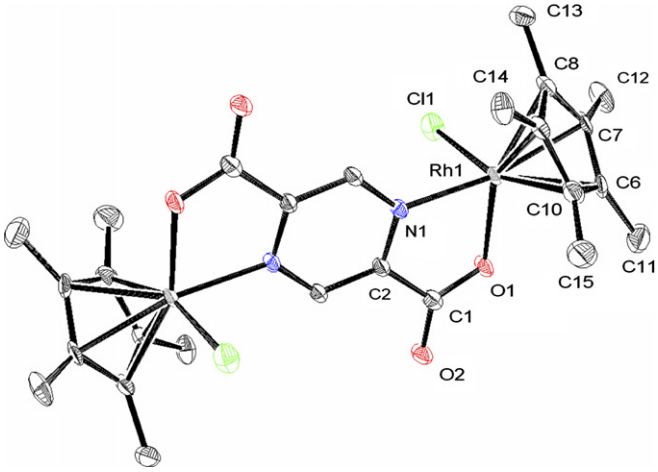

Fig. 4. ORTEP diagram of complex **6** with 50% probability thermal ellipsoids. Hydrogen atoms are omitted for clarity. Selected bond lengths (Å) and angles (°): Rh(1)–Rh(1)^i 6.9996(7), N(1)–Rh(1) 2.132(2), O(1)–Rh(1) 2.099(2), Cl(1)–Rh(1) 2.4086(8); N(1)–Rh(1)–Cl(1) 84.56(7), N(1)–Rh(1)–O(1) 77.71(9), O(1)–Rh(1)–Cl(1) 90.33(7) ($i = 2 - x, 2 - y, -z$).

The unit cell of complex **7** contains two symmetry-independent molecules. The centrosymmetric one is a molecule with *trans* configuration of the two chloro ligands, while the other molecule with a twofold symmetry axis has the two chloro ligands in *cis* configuration, as shown in Fig. 5. Selected bond lengths and angles are presented in Table 1. The ruthenium–chlorine bond distances in the *cis* isomer Ru(2)–Cl(2) 2.388(3) Å and Ru(3)–Cl(3) 2.399(3) Å are slightly shorter than in the *trans* isomer Ru(1)–Cl(1) 2.408(5) Å. The Ru–O bond distances of the *cis* [2.083(10) Å, 2.109(9) Å] and *trans* (2.081(8) Å) molecules are comparable to that of the mononuclear complex **3**.

The UV–Vis data of complexes **1**–**8** and **11**–**12** are listed in Table 2. The low-spin d^6 configuration of the mono and dinuclear complexes provides filled orbitals of proper symmetry at the Ir(III), Rh(III) and Ru(II) centres, which can interact with low-lying π^* orbital of the ligands. One should therefore expect a band attributable to the metal-to-ligand charge transfer (MLCT) ($t_{2g} \rightarrow \pi^*$) transition in their electronic spectra [14]. Furthermore, the energy of these transitions should vary with the nature of the bridging ligand acting as π acceptor [15]. The electronic spectra of the mononuclear complexes **1** and **2** display a medium intensity band in the visible region at ~450 nm and an intense band at ~340 nm. The low intensity band at ~450 nm can be assigned to the metal-to-ligand charge transfer transition (MLCT) ($t_{2g} \rightarrow \pi^*$). The high-energy band at ~340 nm can be assigned to intra-ligand π–π^* transitions. The position of the MLCT transitions in the spectra of the binuclear complexes **7**, **8**, **11** and **12** exhibits significant red shifts (~480 nm) [15]. In general, these complexes follow the normal trends observed in the electronic spectra of the nitrogen bonded metal complexes, which display a ligand based π–π^* transition for pyrazine–carboxylic acid ligands in the UV region and metal-to-ligand charge transfer transitions in the visible region.

2.2. Electrochemistry

The selected complexes [16] have been studied by cyclic voltammetry on a stationary platinum disc and by

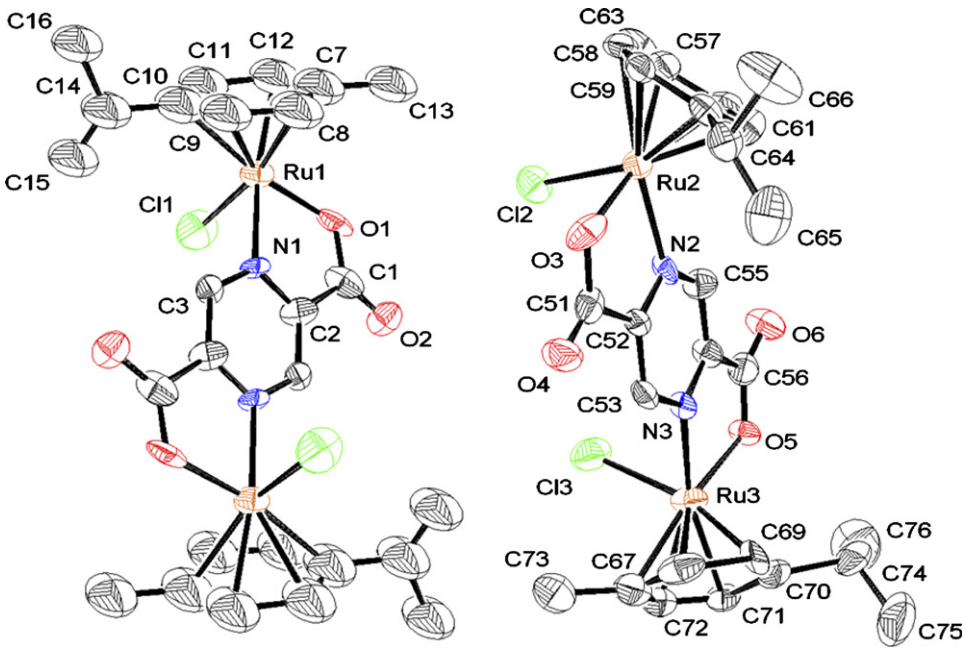

Fig. 5. ORTEP diagram of complex **7**, *trans*-**7** (left) and*cis*-**7** (right), with 50% probability thermal ellipsoids. Hydrogen atoms are omitted for clarity.

Table 1
Selected bond lengths and angles for complex **7**

	trans-**7**	*cis*-**7** (Ru2)	*cis*-**7** (Ru3)
Distances (Å)			
Ru–Cl	2.408(5)	2.388(3)	2.399(3)
Ru–O	2.081(8)	2.083(10)	2.109(9)
Ru–N	2.119(9)	2.102(7)	2.074(7)
Ru–Ru	6.961(2)	6.889(3)	
Angles (°)			
O–Ru–Cl	83.7(3)	86.6(2)	86.1(2)
O–Ru–N	76.8(3)	77.0(4)	76.8(3)
N–Ru–Cl	82.9(3)	84.0(3)	81.6(2)

Table 2
UV–Vis absorption data in acetonitrile at 298 K

Complex		λ_{max}/nm ($\varepsilon/10^{-3}$ M^{-1} cm^{-1})	
1	[(η^5-C_5Me_5)IrCl(L^1)]	456 (0.52)	331 (3.67)
2	[(η^5-C_5Me_5)RhCl(L^1)]		312 (3.16)
3	[(η^6-*p*-Pr^iC_6H_4Me)RuCl(L^1)]	454 (0.55)	340 (3.03)
4	[(η^6-C_6Me_6)RuCl(L^1)]		363 (4.37)
5	[{(η^5-C_5Me_5)IrCl}$_2$(μ-L^2)]	418 (0.85)	
6	[{(η^5-C_5Me_5)RhCl}$_2$(μ-L^2)]	377 (0.81)	
7	[{(η^6-*p*-Pr^iC_6H_4Me)RuCl}$_2$(μ-L^2)]	460 (0.53)	
8	[{(η^6-C_6Me_6)RuCl}$_2$(μ-L^2)]	484 (0.30)	
11	[{(η^6-*p*-Pr^iC_6H_4Me)RuCl}$_2$(μ-L^3)]	436 (0.82)	
12	[{(η^6-C_6Me_6)RuCl}$_2$(μ-L^3)]	464 (0.30)	

voltammetry at a rotating platinum disc electrode (Pt-RDE) in MeCN – 0.1 M NBu_4PF_6 solutions. In our study, we have focused only on the oxidative behaviour since the oxidation is likely to occur at the metal centre. The data are summarised in Table 3.

The mononuclear complexes **1** and **2** exhibit both only one oxidation wave within the experimentally accessible

Table 3
Summary of the electrochemical data[a]

Compound	E_{pa}/E_{pc} [$E_{1/2}$]/[V]
1	+1.46 (irrev.)[b] [+1.45]
2	+1.64 (irrev.)[b] [+1.62]
3	+1.44 (irrev.)[b,c] [+1.43]
4	+1.27/+1.20 [+1.23]
5	+1.52 (irrev.)[b] [+1.53]
6	+1.73 (irrev.)[b]
11	ca. +1.42, +1.50, ca. +1.75 (all irrev.)[b,d,e]
12	ca. +1.23, +1.31, ca. +1.58[b,d,f]

[a] Recorded at platinum electrode in acetonitrile solutions containing 0.1 M Bu_4NPF_6 supporting electrode. E_{pa} and E_{pc} are peak potentials from cyclic voltammetry; $E_{1/2}$ is half-wave potential from voltammetry at RDE. Potentials are given in volts vs. saturated calomel electrode. For irreversible processes, values obtained at 0.1 V s^{-1} scan rate are given.
[b] E_{pa} given.
[c] The electrogenerated product gives rise to a couple of counterwaves at +0.71/+0.77 V.
[d] The separation of the first two waves does not allow for $E_{1/2}$ to be read.
[e] The electrogenerated products gives rise to a pair of waves at ca. +0.68/+0.88 and at +0.84/+1.05 V.
[f] See text.

region, which is attributable to one-electron oxidation of the respective metal centre. In both cases, the oxidation is electrochemically irreversible at 20–500 mV s^{-1} while remaining diffusion-controlled as indicated by $i_p \propto v^{1/2}$ (in cyclic voltammetry) and $i_{lim} \propto \omega^{1/2}$ (in voltammetry at Pt-RDE).[1] In the case of **1**, the oxidation is complicated by adsorption of the electrogenerated species or its decompo-

[1] Definitions: E_{pa} and E_{pc} are anodic and cathodic peak potentials, respectively. Similarly, i_{pa} and i_{pc} denote the anodic and cathodic peak currents. i_{lim} is the limiting voltammetric current, v the scan rate, and ω the rotation frequency of the disc electrode.

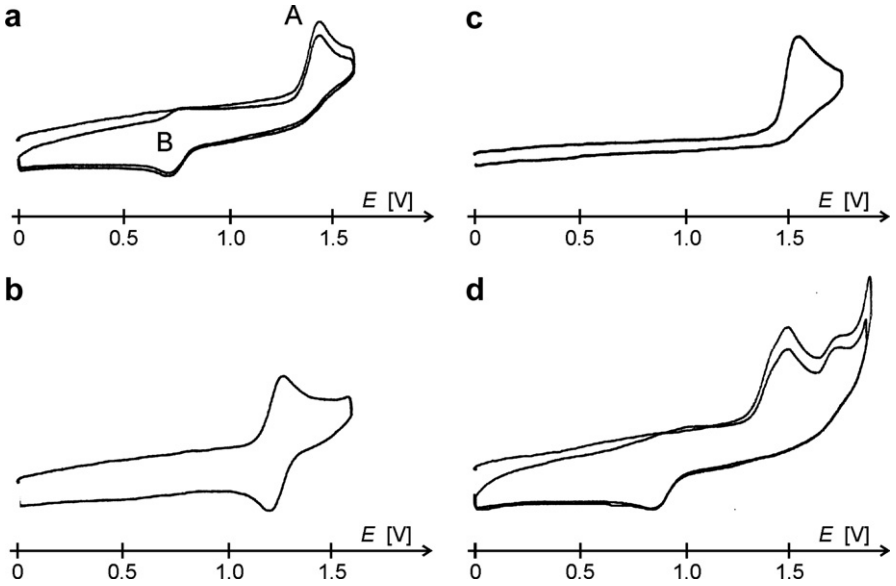

Fig. 6. Cyclic voltammograms of: **3** (a), **4** (b), **5** (c), and **11** (d) recorded at 200 mV s^{-1} (at platinum disc electrode in acetonitrile solutions). The potentials are given relative to saturated calomel electrode.

sition products. However, the processes resulting in coverage of the electrode surface are relatively slow and, therefore, the adsorption phenomena are observable well in voltammograms at Pt-RDE (at 20 mV s^{-1}) whereas in cyclic voltammograms they become apparent only at relatively slow scan rates. Thus, the voltammograms show the expected sigmoidal wave ($E_{1/2}$ + 1.45 V) together with an additional wave at $E_{1/2}$ ca. +1.70 V, whose height also corresponds to one-electron process. By contrast, cyclic voltammograms exert only a single wave (E_{pa} +1.46 V) though with a buckling at the anodic branch of the oxidative half-wave, which becomes more pronounced at slow scan rates.

The redox behaviour of **5** (Fig. 6c) and **6** is similar to their mononuclear counterparts in that both binuclear complexes undergo an irreversible oxidation which is, in the case of the Ir(III) compound, associated with electrode adsorption. The adsorption is manifested in a manner similar to that in **1** (voltammetry vs. cyclic voltammetry), which is again consistent with a relatively slow chemical transformation following the primary electrochemical oxidation to give a product prone to adsorption on the electrode surface. Notably, the heights of the waves in cyclic voltammograms and in voltammograms recorded at Pt-RDE clearly indicate two-electron oxidation processes. This suggests that the oxidation occurs independently and simultaneously at both metal centres present in the molecule, which in turn rules out any significant electronic coupling of the metal-based redox systems (Ir and Rh). As compared with **1** and **2**, the oxidation waves of the binuclear complexes are observed at more positive potentials (ca. 60 and 90 mV). The shift is consistent with the presence of an additional electron-withdrawing carboxyl group on the pyrazine ring and with bridging coordination of the $(L^2)^{2-}$ anion that both reduce the donation per *one* metal centre, thus making the electron removal more difficult.

The redox behaviour of (η^6-arene)ruthenium(II) complexes **3** and **4** (Fig. 6a-b) strikingly differs from that of their Rh(I)- and Ir(I)-analogs and also from each other, even if the compounds differ only by substitution at the arene ring. The redox response of **4** is relatively simple, since the compound is oxidised in a single, practically reversible one-electron step. The oxidation is diffusion-controlled ($i_{pa} \propto v^{1/2}$ and i_{lim}(Pt-RDE) $\propto \omega^{1/2}$) and the i_{pc}/i_{pa} ratio changes from ca. 0.85 to 1.0 upon increasing the scan rate from 20 to 200 mV s^{-1}.

Quite expectedly, the oxidation of compound **3** featuring the less alkylated arene ligand occurs at a potential lower than for **4** – yet, as an irreversible, one-electron process ($i_{pa} \propto v^{1/2}$, i_{lim}(Pt-RDE) $\propto \omega^{1/2}$). However, the primary oxidation (A) is followed by chemical reactions that generate another electroactive species, which gives rise to a couple of peaks (B) at lower potentials in cyclic voltammogram (Fig. 6a). Peak currents associated with the peaks due to the newly formed species (B) are *much* smaller than i_{pa}(A) of the primary oxidation but increase with the scan rate, always holding $i_{pc}(B) < i_{pa}(B)$ at the scan rates applied (N.B. The oxidation counterpeak is hardly observable at rates below ca. 50 mV s^{-1}). The increase of the B-peaks occurs on expense of the primary oxidation (in other words, the primary oxidative peak (or i_{pa}(A)) is higher in the first scan than in the following ones). However, the newly emerged peaks are observed unchanged during repeated cycling. More importantly, the $i_{pc}(B)/i_{pa}(A)$ ratio grows with the scan rate, limiting to 0.5 at 500 mV s^{-1}. Such a behaviour can be explained by a relatively slow formation of a reducible dimeric species after the primary oxidative step.

The increased nuclearity and isomerism in complexes **11** and **12** makes their redox behaviour even more complex. Thus, upon increasing the external potential, compound **12** undergoes three one-electron oxidations: two narrow-spaced steps followed by the third one. The first oxidation is irreversible while the second and third show signs of electrochemical reversibility.

The oxidation of **11** (Fig. 6d) proceeds in a manner similar to that of **12** albeit at potentials by ca. 200 mV higher (see also above). The compound undergoes three subsequent one-electron removals of which the first two are closely separated. Similarly to **3**, the oxidation triggers the formation of a new electroactive species that is observed in the second and following voltammetric cycles as a pair of reductive peaks at around +0.84 and +0.67 V. The peaks become more intense at faster scan rates and after electrolysis at ca. +1.6 V (i.e., after the second oxidative peak) and disappear entirely when the switching potential is set before the main oxidative peak. In contrast to **3**, however, there are no respective oxidative counterparts observed in the cyclovoltammogram of **11**.

The mono- and dinuclear (η^6-arene)ruthenium(II) complexes constitute an interesting set of compounds, which allows for many comparisons. Whereas the oxidation of **4** is practically reversible, that of its *p*-cymene analogue **3** is irreversible, due to some follow-up chemical (structural) changes that probably involve a kind of dimerisation process. The oxidation patterns observed for both binuclear complexes (**11** and **12**) are analogous, too. In both cases, the oxidation proceeds in two one-electron, narrow-spaced waves (RDE) or peaks (CV) followed by a third one; the potentials of the first process corresponding well with the oxidation potentials of the single oxidation process observed for the mononuclear analogues **3** and **4**. The observed small separation of the first two oxidation waves of **11** and **12** indicates certain electronic communication between the metal centres through the bridging ligand (cf. the behaviour of **5** and **6** that feature an isomeric form of the bridging ligand).

In summary, the oxidative patterns seem to be generally analogous for the **3**–**4** and **11**–**12** pairs but strongly influenced by the nature of the aromatic ligands. The substitution at the arene ring not only influences the values of the redox potentials but also affects the overall electrochemical behaviour via governing the reversibility of the electron-transfer reactions and the extent of follow-up chemical reactions. The observed differences between the hexamethylbenzene and *p*-cymene complexes can be rationalised in terms of a higher donor ability and sterically protecting properties of the former arene ligand. Hexamethylbenzene clearly makes the ruthenium centre more electron rich, which is reflected by a shift of the redox potentials to lower values. In addition, however, it better compensates the electron-deficient character of the primary electrogenerated product and hinders its possible structural transformations. Vice versa, the irreversible oxidation as well as the presence of additional waves (though rather minor) due to electrochemically generated product(s) in the voltammograms of (η^6-*p*-cymene)Ru(II) complexes **3** and **11** can be accounted for a relatively lower donating ability and reduced steric bulk.

3. Experimental

3.1. General remarks

All reagents were purchased either from Aldrich or Fluka and used as received. $[\{(\eta^5\text{-}C_5Me_5)MCl_2\}_2]$ (M = Ir, Rh) [17], $[\{(\eta^6\text{-}p\text{-}Pr^iC_6H_4Me)RuCl_2\}_2]$, $[\{(\eta^6\text{-}C_6Me_6)RuCl_2\}_2]$ [18] were prepared according to the literature methods. UV/Vis absorption spectra were recorded on an Uvikon 930 spectrophotometer. CD spectra were recorded on a JASCO J-710 spectropolarimeter (bandwidth 2 nm, step resolution 0.5 nm, response time 4 s, three accumulations). The NMR spectra were recorded on a Varian Gemini 200 MHz or Bruker AMX 400 spectrometer using the residual protonated solvent as internal standard. Infrared spectra were recorded as KBr pellets on a Perkin–Elmer FTIR 1720-X spectrometer. Micro-analyses were performed by the Laboratory of Pharmaceutical Chemistry, University of Geneva (Switzerland). Electrospray mass spectra were obtained in positive-ion mode with an LCQ Finnigan mass spectrometer.

Electrochemical measurements were performed on a multipurpose polarograph PA3 interfaced to a Model 4103 XY recorded (both Laboratorní přístroje, Prague) at room temperature using a standard three-electrode cell: rotating or stationary platinum disc working electrode (1 mm diameter), platinum sheet auxiliary electrode, and saturated calomel electrode (SCE) reference electrode, separated from the analysed solution by a salt bridge filled with 0.1 M Bu_4NPF_6 in acetonitrile. The potential of the reference ferrocene/ferrocenium couple under the experiment conditions was +0.44 V. The samples were dissolved in acetonitrile (Fluka for UV spectroscopy) to give ca. 5×10^{-4} M concentration of the analyte and 0.1 M Bu_4NPF_6 (supporting electrolyte; Fluka, puriss for electrochemistry). The samples were degassed and saturated with argon prior to the measurement and then kept under an argon blanket. Cyclic voltammograms were recorded at stationary platinum disc electrode (scan rates 20–500 mV s^{-1}), while the voltammograms were obtained at rotating disc electrode (500–2500 rpm, scan rates 10–100 mV s^{-1}).

3.2. Synthesis of the mononuclear complexes *1–4*

Sodium methoxide (17.3 mg, 0.32 mmol) and pyrazine-2-carboxylic acid (39.7 mg, 0.32 mmol) were added to a suspension of the corresponding dimeric chloro complex (0.16 mmol) in dry methanol (20 ml). Then the suspension was stirred at room temperature for 6 h. During the period the starting materials dissolved completely, and the solution became first of all clear. In the second half of the reac-

tion time the solution became cloudy again, as the product precipitated. The precipitate was filtered, washed three times with diethylether (3 × 10 ml) and then dried *in vacuo.*

*3.2.1. [(η^5-C_5Me_5)IrCl(L^1)] (**1**)*

Yellow solid, yield 116 mg, (75%). ^{1}H NMR (CD_2Cl_2, 200 MHz): 9.18 (d, 1H, $^4J = 1.10$ Hz, Pz-$H_{\beta'}$), 8.83 (d, 1H, $^3J = 2.92$ Hz, Pz-H_α), 8.50 (dd, 1H, Pz-H_β), 1.68 (s, 15H, C_5Me_5). IR (cm^{-1}): 1656(s) (COO). ESI-MS: 509.1 [M+Na]$^+$. Anal. Calc. for (%): $C_{15}H_{18}N_2ClO_2Ir$: C, 37.07; H, 3.73; N, 5.76. Found: C, 37.03; H, 3.49; N, 5.50%.

*3.2.2. [(η^5-C_5Me_5)RhCl(L^1)] (**2**)*

Orange-yellow solid, yield 91 mg, (72%). ^{1}H NMR (CD_2Cl_2, 200 MHz): 9.15 (d, 1H, $^4J = 1.46$ Hz, Pz-$H_{\beta'}$), 8.87 (d, 1H, $^3J = 2.92$ Hz, Pz-H_α), 8.51 (dd, 1H, Pz-H_β), 1.70 (s, 15H, C_5Me_5). IR (cm^{-1}): 1648(s) (COO). ESI-MS: 419.0 [M+Na]$^+$. Anal. Calc. for (%): $C_{15}H_{18}N_2ClO_2Rh$: C, 45.42; H, 4.57; N, 7.06. Found: C, 45.85; H, 4.78; N, 6.93%.

*3.2.3. [(η^6-p-$Pr^iC_6H_4Me$)RuCl(L^1)] (**3**)*

Orange-yellow solid, yield 95 mg, (74%). ^{1}H NMR (CD_2Cl_2, 400 MHz): 9.11 (d, 1H, $^4J = 1.20$ Hz, Pz-$H_{\beta'}$), 8.93 (dd, 1H, $^3J = 3.04$ Hz, Pz-H_β), 8.85 (d, 1H, Pz-H_α), 5.69 (d, 1H, $^3J = 6.00$ Hz, $Ar_{p\text{-cym}}$), 5.67 (d, 1H, $^3J = 6.00$ Hz, $Ar_{p\text{-cym}}$), 5.53 (d, 1H, $Ar_{p\text{-cym}}$), 5.49 (d, 1H, $Ar_{p\text{-cym}}$), 2.89 (sep, 1H, $^3J = 3.72$ Hz, $CH(CH_3)_2$), 2.16 (s, 3H, CH_3), 1.30 (d, 3H, $CH(CH_3)_2$), 1.29 (d, 3H, $CH(CH_3)_2$). IR (cm^{-1}): 1658(s) (COO). ESI-MS: 416.9 [M+Na]$^+$. Anal. Calc. for (%): $C_{15}H_{17}N_2ClO_2Ru$: C, 45.86; H, 4.36; N, 7.13. Found: C, 45.45; H, 4.27; N, 7.02%.

*3.2.4. [(η^6-C_6Me_6)RuCl(L^1)] (**4**)*

Orange solid, yield 110 mg, (81%). ^{1}H NMR (CD_2Cl_2, 400 MHz): 9.05 (d, 1H, $^4J = 1.20$ Hz, Pz-$H_{\beta'}$), 8.83 (d, 1H, $^3J = 3.07$ Hz, Pz-H_α), 8.63 (dd, 1H, Pz-H_β), 2.18 (s, 18H, C_6Me_6). IR (cm^{-1}): 1659(s) (COO). ESI-MS: 445.0 [M+Na]$^+$. Anal. Calc. for (%): $C_{17}H_{21}N_2ClO_2Ru$: C, 48.35; H, 5.01; N, 6.64. Found: C, 48.70; H, 5.03; N, 6.46%.

*3.3. Synthesis of the dinuclear complexes **5**–**8***

Sodium methoxide (17.3 mg, 0.32 mmol) and pyrazine-2-carboxylic acid (27 mg, 0.16 mmol) were added to a suspension of the corresponding dimeric chloro complex (0.16 mmol) in dry methanol (20 ml). Then the suspension was stirred at room temperature for 3 h. During the period the starting materials dissolved completely, and the solution became first of all clear. In the second half of the reaction time the solution became cloudy again, as the product precipitated. The precipitate was filtered, washed three times with diethylether (3 × 10 ml) and then dried *in vacuo.*

*3.3.1. [{(η^5-C_5Me_5)IrCl}$_2$(μ-L^2)] (**5**)*

Orange solid, yield 114 mg, (80%). ^{1}H NMR (CD_2Cl_2, 200 MHz): 9.03 (s, 2H, Pz), 1.70 (s, 30H, C_5Me_5). IR (cm^{-1}): 1673(s) (COO). ESI-MS: 915.1 [M+Na]$^+$. Anal. Calc. for (%): $C_{26}H_{32}N_2Cl_2O_4Ir_2$: C, 35.01; H, 3.61; N, 3.14. Found: C, 35.32; H, 3.72; N, 3.12%.

*3.3.2. [{(η^5-C_5Me_5)RhCl}$_2$(μ-L^2)] (**6**)*

Orange-yellow solid, yield 104 mg, (91%). ^{1}H NMR (CD_2Cl_2, 200 MHz): 9.05 (s, 2H, Pz), 1.71 (s, 30H, C_5Me_5). IR (cm^{-1}): 1656(s) (COO). ESI-MS: 735.0 [M+Na]$^+$. Anal. Calc. for (%): $C_{26}H_{32}N_2Cl_2O_4Rh_2$: C, 43.78; H, 4.52; N, 3.93. Found: C, 43.98; H, 4.80; N, 3.49%.

*3.3.3. [{(η^6-p-$Pr^iC_6H_4Me$)RuCl}$_2$(μ-L^2)] (**7**)*

Orange solid, yield 95 mg, (82%). ^{1}H NMR ($CDCl_3$, 400 MHz): 9.31 (s, 2H, Pz), 5.72 (d, 2H, $^3J = 5.64$ Hz, $Ar_{p\text{-cym}}$), 5.70 (d, 2H, $^3J = 5.64$ Hz, $Ar_{p\text{-cym}}$), 5.59 (d, 2H, $Ar_{p\text{-cym}}$), 5.56 (d, 2H, $Ar_{p\text{-cym}}$), 2.95 (sep, 2H, $^3J_{H-H} = 3.84$ Hz, $CH(CH_3)_2$), 2.33 (s, 6H, CH_3), 1.32 (d, 6H, $CH(CH_3)_2$), 1.29 (d, 6H, $CH(CH_3)_2$). IR (cm^{-1}): 1654(s) (COO). Mass (ESI): 730.9 [M+Na]$^+$. Anal. Calc. for (%): $C_{26}H_{30}N_2Cl_2O_4Ru_2$: C, 44.13; H, 4.27; N, 3.95. Found: C, 44.65; H, 4.71; N, 3.62%.

*3.3.4. [{(η^6-C_6Me_6)RuCl}$_2$(μ-L^2)] (**8**)*

Red solid, yield 64 mg, (53%). ^{1}H NMR (CD_2Cl_2, 400 MHz): 8.98 (s, 2H, Pz), 2.17 (s, 36H, C_6Me_6). IR (cm^{-1}): 1658(s) (COO). Mass (ESI): 787.0 [M+Na]$^+$. Anal. Calc. for (%): $C_{30}H_{38}N_2Cl_2O_4Ru_2$: C, 47.18; H, 5.01; N, 3.66. Found: C, 47.63; H, 5.16; N, 3.30%.

*3.4. Synthesis of the dinuclear complexes **9**–**12***

Sodium methoxide (17.3 mg, 0.32 mmol) and pyrazine-2-carboxylic acid (27 mg, 0.16 mmol) were added to a suspension of the corresponding dimeric chloro complex (0.16 mmol) in dry methanol (20 ml). Then the suspension was stirred at room temperature for 3 h. During the period the starting materials dissolved completely, and the solution became first of all clear. In the second half of the reaction time the solution became cloudy again, as the product precipitated. The precipitate was filtered, washed three times with diethylether (3 × 10 ml) and then dried *in vacuo.*

*3.4.1. [{(η^5-C_5Me_5)IrCl}$_2$(μ-L^3)] (**9**)*

Red solid, yield 116 mg, (82%). IR (cm^{-1}): 1690 (s), 1665 (s) (COO). Mass (ESI): 915.1 [M+Na]$^+$. Anal. Calc. for (%): $C_{26}H_{32}N_2Cl_2O_4Ir_2$: C, 35.01; H, 3.61; N, 3.14. Found: C, 35.59; H, 3.64; N, 3.00%.

*3.4.2. [{(η^5-C_5Me_5)RhCl}$_2$(μ-L^3)] (**10**)*

Orange-yellow solid, yield 96 mg, (84%). IR (cm^{-1}): 1678 (s), 1654 (s) (COO). Mass (ESI): 736.27 [M+Na]$^+$. Anal. Calc. for (%): $C_{26}H_{32}N_2Cl_2O_4Rh_2$: C, 43.78; H, 4.52; N, 3.93. Found: C, 43.22; H, 4.62; N, 3.78%.

*3.4.3. [{(η^6-p-$Pr^iC_6H_4Me$)RuCl}$_2$(μ-L^3)] (**11**)*

Orange-yellow solid, yield 78 mg, (67%). ^{1}H NMR (CD_3CN, 200 MHz): 9.12 (s, 2H, Pz), 5.76 (d, 2H,

Table 4
Crystallographic and structure refinement parameters for complexes **2**, **3**, **5** · $2CH_2Cl_2$, **6** · $2CH_2Cl_2$ and **7**

	2	**3**	**5** · $2CH_2Cl_2$	**6** · $2CH_2Cl_2$	**7**
Chemical formula	$C_{15}H_{18}ClN_2O_2Rh$	$C_{15}H_{17}ClN_2O_2Ru$	$C_{28}H_{36}Cl_6Ir_2N_2O_4$	$C_{26}H_{36}Cl_6N_2O_4Rh_2$	$C_{26}H_{30}Cl_2N_2O_4Ru_2$
Formula weight	396.67	393.83	1061.69	883.11	707.56
Crystal system	Orthorhombic	Monoclinic	Monoclinic	Monoclinic	Monoclinic
Space group	$P2_12_12_1$ (no. 19)	$P2_1/n$ (no. 14)	$P2_1/n$ (no. 14)	$P2_1/n$ (no. 14)	$C2/c$ (no. 15)
Crystal colour and shape	Orange block	Brown rod	Red rod	Orange rod	Orange block
Crystal size	$0.28 \times 0.20 \times 0.20$	$0.40 \times 0.15 \times 0.15$	$0.55 \times 0.10 \times 0.10$	$0.50 \times 0.20 \times 0.20$	$0.22 \times 0.10 \times 0.10$
a (Å)	7.828(2)	6.0024(7)	7.9512(6)	7.9544(7)	22.741(5)
b (Å)	9.183(2)	16.642(2)	9.4388(7)	9.3868(6)	21.095(4)
c (Å)	21.297(4)	15.428(2)	22.6265(17)	22.588(2)	20.103(4)
β (°)	90	100.544(16)	90.323(9)	90.601(11)	110.16(3)
V (Å^3)	1530.9(6)	1515.1(3)	1698.1(2)	1686.5(2)	9053(3)
Z	4	4	2	2	12
T (K)	173(2)	173(2)	173(2)	173(2)	173(2)
D_c (g cm^{-3})	1.721	1.726	2.076	1.739	1.557
μ (mm^{-1})	1.295	1.216	8.337	1.490	1.209
Scan range (°)	$2.42 < \theta < 25.86$	$2.45 < \theta < 26.04$	$2.34 < \theta < 25.94$	$2.35 < \theta < 25.44$	$1.93 < \theta < 26.02$
Unique reflections	2950	2942	3284	3256	7467
Reflections used [$I > 2\sigma(I)$]	2821	1815	2902	2811	2378
R_{int}	0.1077	0.1263	0.0659	0.1176	0.0856
Final R indices [$I > 2\sigma(I)$][a]	0.0435, wR_2 0.1149	0.0619, wR_2 0.1472	0.0292, wR_2 0.0702	0.0343, wR_2 0.0864	0.0613, wR_2 0.1285
R indices (all data)	0.0492, wR_2 0.1571	0.0970, wR_2 0.1762	0.0338, wR_2 0.0734	0.0395, wR_2 0.0979	0.1824, wR_2 0.1495
Goodness-of-fit	1.184	0.891	1.046	1.074	0.701
Maximum, minimum $\Delta\rho/e$ (Å^{-3})	1.424, −2.648	1.578, −2.090	0.973, −1.268	0.881, −1.948	2.070, −0.884

[a] Structures were refined on F_0^2: $wR_2 = [\sum[w(F_0^2 - F_c^2)^2]/\sum w(F_0^2)^2]^{1/2}$, where $w^{-1} = [\sum(F_0^2) + (aP)^2 + bP]$ and $P = [\max(F_0^2, 0) + 2F_c^2]/3$.

$^3J = 3.66$ Hz, $Ar_{p\text{-cym}}$), 5.73 (d, 2H, $^3J = 3.66$ Hz, $Ar_{p\text{-cym}}$), 5.59 (d, 2H, $Ar_{p\text{-cym}}$), 5.56 (d, 2H, $Ar_{p\text{-cym}}$), 2.82 (sep, 2H, $^3J_{H-H} = 4.76$ Hz, $CH(CH_3)_2$), 2.16 (s, 6H, CH_3), 1.27 (d, 6H, $CH(CH_3)_2$), 1.23 (d, 6H, $CH(CH_3)_2$). IR (cm^{-1}): 1678(s), 1657(s) (COO). Mass (ESI): 731.0 $[M+Na]^+$. Anal. Calc. for (%): $C_{26}H_{30}N_2Cl_2O_4Ru_2$: C, 44.13; H, 4.27; N, 3.95. Found: C, 44.72; H, 4.38; N, 3.80%.

3.4.4. $[\{(\eta^6\text{-}C_6Me_6)RuCl\}_2(\mu\text{-}L^3)]$ (**12**)

Orange-yellow solid, yield 86 mg, (70%). ^{1}H NMR (CD_2Cl_2, 200 MHz): 8.58 (s, 2H, Pz), 2.09 (s, 36H, C_6Me_6). IR (cm^{-1}): 1687(s), 1662(s) (COO). Mass (ESI): 764.9 $[M+Na]^+$. Anal. Calc. for (%): $C_{30}H_{38}N_2Cl_2O_4Ru_2$: C, 47.18; H, 5.01; N, 3.66. Found: C, 47.42; H, 5.10; N, 3.57%.

3.5. X-ray crystallography

Crystals of complexes **2**, **3**, **5**, **6** and **7** were mounted on a Stoe Image Plate Diffraction system equipped with a ϕ circle goniometer, using Mo Kα graphite monochromated radiation ($\lambda = 0.71073$ Å) with ϕ range 0–200°. The structures were solved by direct methods using the program SHELXS-97 [19]. Refinement and all further calculations were carried out using SHELXL-97 [20]. The H-atoms were included in calculated positions and treated as riding atoms using the SHELXL default parameters. The non-H atoms were refined anisotropically, using weighted full-matrix least-square on F^2. Crystallographic details are summarised in Table 4. Figures of complex **2**–**3** and **5**–**7** were drawn with ORTEP-32 [21].

Acknowledgements

Financial support from the Fonds National Suisse de la Recherche Scientifique is gratefully acknowledged. This work is also a part of the research projects of the Czech Ministry of Education, Youth and Sports (Projects LC510, "Research Center of Nanotechnology and Nanoelectronics" and LC06070, "Center for Structure and Synthetic Application of Transition Metal Complexes"). A generous loan of ruthenium chloride hydrate from the Johnson Matthey Technology Centre is gratefully acknowledged.

Appendix A. Supplementary material

CCDC 622205, 522206, 622207, 622208, and 622209 contain the supplementary crystallographic data for **2**, **3**, **5** · $2CH_2Cl_2$, **6** · $2CH_2Cl_2$, and **7**. These data can be obtained free of charge via http://www.ccdc.cam.ac.uk/conts/retrieving.html, or from the Cambridge Crystallographic Data Centre, 12 Union Road, Cambridge CB2 1EZ, UK; fax: (+44) 1223-336-033; or e-mail: deposit@ccdc.cam.ac.uk. Supplementary data associated with this article can be found, in the online version, at doi:10.1016/j.jorganchem.2006.12.040.

References

[1] M. Fujita, J. Yazaki, K. Ogura, J. Am. Chem. Soc. 112 (1990) 5645.
[2] (a) C.J. Kuehl, S.D. Huang, P.J. Stang, J. Am. Chem. Soc. 123 (2001) 9634;

(b) T. Moriuchi, M. Miyaishi, T. Hirai, Angew. Chem. Int. Ed. 40 (2001) 3042;
(c) N. Das, P.S. Mukherjee, A.M. Arif, P.J. Stang, J. Am. Chem. Soc. 125 (2003) 13950;
(d) P.S. Mukherjee, N. Das, Y.K. Kryschenko, A.M. Arif, P.J. Stang, J. Am. Chem. Soc. 126 (2004) 2464;
(e) D.C. Caskey, R.K. Shoemaker, J. Michl, Org. Lett. 6 (2004) 2093;
(f) M. Yoshizawa, M. Nagao, K. Kumazawa, M. Fujita, J. Organomet. Chem. 690 (2005) 5383;
(g) D. Kim, J.H. Paek, M.-J. Jun, J.Y. Lee, S.O. Kang, J. Ko, Inorg. Chem. 44 (2005) 7886.

[3] M. Fujita, D. Oguro, M. Miyazawa, H. Oka, K. Yamaguchi, K. Ogura, Nature 378 (1995) 469.

[4] (a) L. Pirondini, F. Bertolini, B. Cantadori, F. Ugozzoli, C. Massera, E. Dalcanale, Proc. Natl. Acad. Sci. USA 99 (2002) 4911, and references therein;
(b) M.V. Ovchinnikov, B.J. Holliday, C.A. Mirkin, L.N. Zakharov, A.L. Rheingold, Proc. Natl. Acad. Sci. USA 99 (2002) 4927, and references therein;
(c) C.J. Kuehl, Y.K. Kryschenko, U. Radhakrishnan, S. Russell Seidel, S.D. Huang, P.J. Stang, Proc. Natl. Acad. Sci. USA 99 (2002) 4932, and references therein;
(d) C.J. Kuehl, T. Yamamoto, S. Russell Seidel, P.J. Stang, Org. Lett. 4 (2002) 913;
(e) Y.K. Kryschenko, S. Russell Seidel, D.C. Muddiman, A.I. Nepomuceno, P.J. Stang, J. Am. Chem. Soc. 125 (2003) 9647;
(f) J.D. Crowley, A.J. Goshe, B. Bosnich, Chem. Commun. (2003) 2824;
(g) M. Fujita, M. Tominaga, A. Hori, B. Therrien, Acc. Chem. Res. 38 (2005) 369, and references therein;
(h) D.C. Caskey, J. Michl, J. Org. Chem. 70 (2005) 5442;
(i) V. Maurizot, M. Yoshizawa, M. Kawano, M. Fujita, Dalton Trans. (2006) 2750.

[5] (a) H. Yan, G. Süss-Fink, A. Neels, H. Stoeckli-Evans, J. Chem. Soc., Dalton Trans. (1997) 4345;
(b) K.D. Benkstein, J.T. Hupp, C.L. Stern, J. Am. Chem. Soc. 120 (1998) 12982;
(c) S.M. Woessner, J.B. Helms, Y. Shen, B.P. Sullivan, Inorg. Chem. 37 (1998) 5406;
(d) S. Roche, C. Haslam, H. Adams, S.L. Heath, J.A. Thomas, Chem. Commun. (1998) 1681;
(e) T. Rajendran, B. Manimaran, F.-Y. Lee, G.-H. Lee, S.-M. Peng, C.M. Wang, K.-L. Lu, Inorg. Chem. 39 (2000) 2016;
(f) S.-S. Sun, A.J. Lees, Chem. Commun. (2001) 103;
(g) F.A. Cotton, C. Lin, C.A. Murillo, Acc. Chem. Res. 34 (2001) 759, and references therein;
(h) S.-S. Sun, A.J. Lees, Inorg. Chem. 40 (2001) 3154;
(i) P.S. Mukherjee, K.S. Min, A.M. Arif, P.J. Stang, Inorg. Chem. 43 (2004) 6345;
(j) A.H. Mahmoudkhani, A.P. Côté, G.K.H. Shimizu, Chem. Commun. (2004) 2678.

[6] K. Severin, Chem. Commun. (2006) 3859, and references therein.

[7] (a) H. Piotrowski, K. Polborn, G. Hilt, K. Severin, J. Am. Chem. Soc. 123 (2001) 2699;
(b) H. Piotrowski, G. Hilt, A. Schulz, P. Mayer, K. Polborn, K. Severin, Chem. Eur. J. 7 (2001) 3197.

[8] D.P. Smith, E. Baralt, B. Morales, M.M. Olmstead, M.F. Maestre, R.H. Fish, J. Am. Chem. Soc. 114 (1992) 10647.

[9] P. Govindaswamy, D. Linder, J. Lacour, G. Süss-Fink, B. Therrien, Chem. Commun. (2006) 4691.

[10] D. Sukanya, R. Prabhakaran, K. Natarajan, Polyhedron 25 (2006) 2223.

[11] (a) H. Brunner, B. Nuber, M. Prommesberger, Tetrahedron: Asymmetry 9 (1998) 3223;
(b) H. Brunner, M. Weber, M. Zabel, Coord. Chem. Rev. 242 (2003) 3;
(c) H. Brunner, A. Kollnberger, A. Mehmood, T. Tsuno, M. Zabel, Organometallics 23 (2004) 4006;
(d) A.J. Davenport, D.L. Davies, J. Fawcett, D.R. Russell, Dalton Trans. (2004) 1481;
(e) J.V. Craenenbroeck, K.V. Isterdael, C. Vercaemst, F. Verpoort, New J. Chem. 29 (2005) 942;
(f) D. Zuccaccia, E. Clot, A. Macchioni, New J. Chem. 29 (2005) 430;
(g) P. Peach, D.J. Cross, J.A. Kenny, I. Mann, I. Houson, L. Campbell, T. Walsgrove, M. Wills, Tetrahedron 62 (2006) 1864;
(h) A.J. Davenport, D.L. Davies, J. Fawcett, D.R. Russell, J. Organomet. Chem. 691 (2006) 2221.

[12] (a) H. Brunner, A. Kollnberger, T. Burgemeister, M. Zabel, Polyhedron 19 (2000) 1519;
(b) P. Govindaswamy, M.R. Kollipara, J. Coord. Chem. 59 (2006) 131.

[13] H. Aneetha, P.S. Zacharias, B. Srinivas, G.H. Lee, Y. Wang, Polyhedron 18 (1999) 299.

[14] (a) N. Goswami, R. Alberto, C.L. Barnes, S. Jurisson, Inorg. Chem. 35 (1996) 7546;
(b) R. Samanta, P. Munshi, B.K. Santra, N.K. Lokanath, M.A. Sridhar, J.S. Prasad, G.K. Lahiri, J. Organomet. Chem. 579 (1999) 311;
(c) P.K. Santra, C. Sinha, W.-J. Sheen, F.-L. Liao, T.-H. Lu, Polyhedron 20 (2001) 599;
(d) A.K. Ghosh, K.K. Kamar, P. Paul, S.-M. Peng, G.-H. Lee, S. Goswami, Inorg. Chem. 41 (2002) 6343;
(e) C. Das, A.K. Ghosh, C.-H. Hung, G.-H. Lee, S.-M. Peng, S. Goswami, Inorg. Chem. 41 (2002) 7125;
(f) S. Jasimuddin, T. Mathur, C. Sinha, Inorg. Chim. Acta 358 (2005) 3601.

[15] (a) D.W. Herlocker, R.S. Drago, V.I. Meek, Inorg. Chem. 5 (1966) 2009;
(b) R.E. Clarke, P.C. Ford, Inorg. Chem. 9 (1970) 495;
(c) J.M. Malin, C.F. Schmidt, H.E. Toma, Inorg. Chem. 14 (1975) 2924;
(d) D.K. Lavallee, M.D. Baughman, M.P. Phillips, J. Am. Chem. Soc. 99 (1977) 718;
(e) N.G. Del, V. Morena, N.E. Katz, J. Olabe, P.J. Aymonino, Inorg. Chim. Acta 35 (1979) 183.

[16] Complexes, **7**–**10**, are practically insoluble in MeCN, which made an electrochemical study impossible.

[17] (a) J.W. Kang, K. Moseley, P.M. Maitlis, J. Am. Chem. Soc. 91 (1969) 5970;
(b) R.G. Ball, W.A.G. Graham, D.M. Heinekey, J.K. Hoyano, A.D. McMaster, B.M. Mattson, S.T. Michel, Inorg. Chem. 29 (1990) 2023;
(c) C. White, A. Yates, P.M. Maitlis, Inorg. Synth. 29 (1992) 228.

[18] (a) M.A. Bennett, A.K. Smith, J. Chem. Soc., Dalton Trans. (1974) 233;
(b) M.A. Bennett, T.W. Matheson, G.B. Robertson, A.K. Smith, P.A. Tucker, Inorg. Chem. 19 (1980) 1014;
(c) M. A Bennett, T.N. Huang, T.W. Matheson, A.K. Smith, Inorg. Synth. 21 (1982) 74.

[19] G.M. Sheldrick, Acta Cryst. A46 (1990) 467.

[20] G.M. Sheldrick, SHELXL-97, University of Göttingen, Göttingen, Germany, 1999.

[21] L.J. Farrugia, J. Appl. Cryst. 30 (1997) 565.